ACTA METALLURGICA SLOVACA
2024, VOL. 30, NO. 1, 19-23

RESEARCH PAPER

MICROSTRUCTURE OF THE P92 WELD JOINT AFTER 5000 H OF ANNEALING

Sroka Marek [1], Sówka Karola [1,2], Purzyńska Hanna [3], Puszczało Tomasz [1,2] , Zieliński Adam [3]

[1] Silesian University of Technology, Department of Engineering Materials and Biomaterials, S. Konarskiego 18A, 44-100 Gliwice, Poland
[2] ZRE Katowice, 13 Gen. Jankego Str., 40-615 Katowice, Poland
[3] Lukasiewicz Research Network – Upper Silesian Institute of Technology, K. Miarki 12-14, 44-100 Gliwice, Poland

* Corresponding author: marek.sroka@polsl.pl, Silesian University of Technology, Department of Engineering Materials and Biomaterials, S. Konarskiego 18A, 44-100 Gliwice, Poland.

Received: 29.01.2021
Accepted: 03.03.2024

ABSTRACT

P92 (X10CrWMoVNb9-2) is commonly used for high-pressure elements of modern power units for supercritical steam parameters. As a result, steel is characterized by good strength, corrosion and creep resistance properties at elevated temperatures. Welded joints of pressure elements of steam boilers are potentially the weakest points in assessing their service life. Therefore, they are a place where, during long-term operation, the continuity of the material within the weld, usually in the heat-affected zone, may be lost. Therefore, material studies of welded joints on the base material contribute to the understanding of degradation processes. The paper presents microstructure and hardness testing of the P92 welded joint after 5000h of annealing at 600 and 650°C. The hardness of the material was compared to the microstructure images in the initial state and after annealing. A scanning electron microscope carried out the microstructure tests.

Keywords: microstructure, creep, pipe, weld, lifetime, P92.

INTRODUCTION

As the world grapples with mounting energy demands and stringent environmental standards set by global authorities, the modernization of power plant units becomes paramount. One avenue to elevate production efficiency is by elevating the steam parameters within the power block. This, in turn, mandates upgrading pressure components to align with these enhanced operational parameters. Elevating these parameters invariably necessitates the deployment of materials boasting superior strength and creep resistance [1,2]. For 1000 MW power units operating under 300 bars and 630°C steam parameters, X10CrWMoVNb9-2 steel, commonly known as P92 steel, stands out [3]. This steel, recognized for its exceptional creep resistance, oxidation resistance, and diminished thermal expansion coefficient, has become preferred for thick-walled components like main steam pipelines, headers, and heat exchangers. P92 steel's evolution from its precursor, P91 steel, involved strategic chemical modifications, including adding W and micro-additions of N and B. These compositional tweaks have enhanced its corrosion and creep resistance, making it highly attractive for use [4-6].
However, challenges persist. This paper focused on the welds representing the most vulnerable points in components, with creep emerging as a dominant degradation mechanism. Assessment of the condition of welded joints is crucial for the safe operation of power plants [7-9]. The research aims to compare welded joint microstructure and microstructure hardness of the initial state after annealing in high-temperature conditions.

MATERIAL AND METHODS

Materials

T/P92 steel tubes produced by Vallourec Mannesmann France, with an outside diameter of Ø88.9 mm and wall thickness of 17.5 mm, were used to prepare specimens. The tubes were hot rolled at the mill, normalized at 1060°C for 20 minutes, followed by air cooling, and finally tempered at 770°C for 60 minutes, followed by air cooling. Material chemical composition according to standard EN10216-2:2013 and filler materials are presented in **Table 1**. The chosen pipe ratio between the diameter and thickness aligns with the proportions of thick-walled pipes used at modern high-pressure pipelines designed for supercritical parameters.

Welding

Pipes were cut into 200 mm sections and machined to the requested welding detail. Tubes were welded at the root layer of the welded joint using the GTAW (Gas Tungsten Arc Welding) method, and the filling and facing layers were applied using the SMAW (Shielded Metal Arc Welding) approach. These two methods are widely employed in fabricating high-pressure components for the energy sector, and the pressure piping standards also confirm this. The welding process utilized metal wires, in compliance with PN-EN ISO 21952, along with electrodes, following the guidelines of PN-EN ISO 3580. The chemical composition percentages of the materials employed in the welding procedure are presented in **Table 1**. Welding was carried out at interpass temperatures at 200-250°C then cooled in air. After that, the post-welding heat treatment at 750°C within 60 minutes has been done.

Table 1 Chemical composition for tested P92 welding joint [%wt.].

EN 10216-2: Seamless steel tubes for pressure purposes - X10CrWMoVNb9-2

C	Si	Mn	P max	S max	Nb	Ti	V	Zr
0.07 to 0.13	≤ 0.50	0.30 to 0.60	0.02	0.01	0.04 to 0.09	0.01 max	0.15 to 0.25	0.01 max
Cr	**Mo**	**Ni**	**N**	**B**	**Al tot**	**Cu**		**W**
8.5 to 9.5	0.30 to 0.60	≤ 0.40	0.030 to 0.070	0.001 to 0.006	≤ 0.02	-		1.50 to 2.00

EN ISO 3580: Covered electrodes for manual metal arc welding of creep-resisting steels - X10CrWMoVNb9-2

C	Si	Mn	Cr	Ni	Mo	V	Nb	W	N
0.1	0.3	0.5	8.6	0.5	0.4	0.2	0.05	1.50	0.05

EN ISO 21952: Wire electrode, wires, rods and deposits for gas-shielded arc welding of creep-resisting steels - X10CrWMoVNb9-2

C	Si	Mn	Cr	Mo	Ni	W	V	N	Nb
0.1	0.3	0.7	8.6	0.55	0.7	1.6	0.20	0.04	0.04

Methods

The tests were performed for the material of the initial state and after annealing at 600°C for 5000h and 650°C for 5000h. Specimens and annealing were performed at Lukasiewicz Research Network – Upper Silesian Institute of Technology in Gliwice.

The microstructural analysis of the joint made of P92 steel was carried out on metallographic specimens revealing the joint zones: parent material, heat-affected zone and weld metal. Metallographic specimens were made on the pipe joints' cross-section by grinding, mechanical polishing, and etching. The microstructure was reviewed using the Inspect F scanning electron microscope at a magnification of up to 5000x.

The hardness evaluations of the weld joint were conducted using a Zwick Z250 test apparatus with a top force of 250 kN. Specimens were examined following the guidelines of PN-EN ISO 6892-1:2016-09. Hardness tests were executed on initial weld joint specimens and those post-annealed for 5000h at 600°C and 650°C.

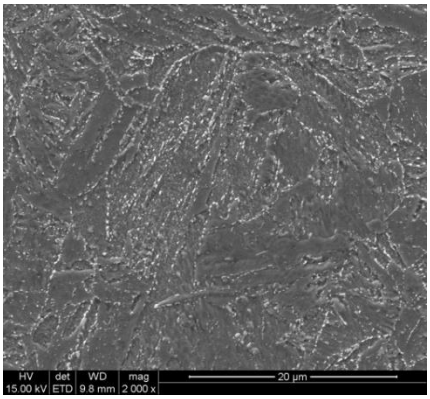

Fig. 1 Parent material - initial state

RESULTS AND DISCUSSION

Welded joint - initial state

The microstructure tests of a similar welded joint were divided into zones following the discussed scheme PM (Parent material)/HAZ (Heat affected zone)/WM (Weld metal). Observations of the parent material for both sides of the joint showed the microstructure of tempered martensite with very fine precipitates of the $M_{23}C_6$ type on the former austenite grain boundaries and martensite laths, which is characteristic of the initial state of the tested steel (**Fig. 1**). Observations of the heat affected zone for both sides of the joints showed a fine-grained microstructure of tempered martensite with numerous precipitates on the former austenite grain boundaries and martensite laths. In the tested zone, no discontinuities and microcracks in the microstructure were found (**Fig. 2**) and in the weld metal zone (**Fig. 3**).

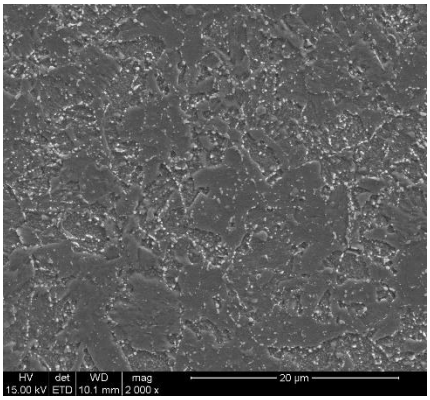

Fig. 2 Heat affected zone - initial state

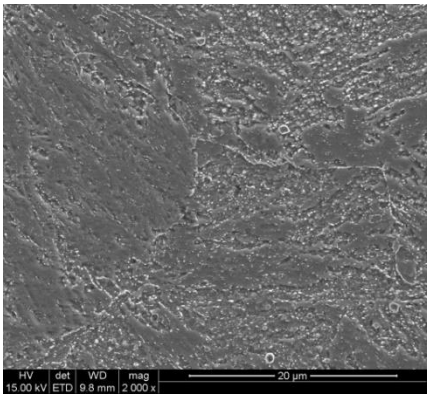

Fig. 3 Weld metal - initial state

Welded joint - after annealing for 5000h in 600°C

Studies of the microstructure of a similar welded joint after annealing at 600ºC were also divided into zones PM/HAZ/WM. Observations of the parent material for both sides of the joint using a scanning electron microscope showed a microstructure very similar to the initial state (**Fig. 4**), i.e. the microstructure of tempered strip martensite with a noticeable, however, a very slight increase in the size of the precipitates, mainly along the grain boundaries of the former austenite.

Observations of the microstructure for both sides of the heat-affected zone (**Fig. 5**) showed a fine-grained microstructure of tempered martensite with numerous precipitates on the grain boundaries of the former austenite and martensite strips, which does not differ from the initial state in the HAZ of the tested welded joint. Microstructure observations for the weld zone (**Fig. 6**) did not show any noticeable changes in the microstructure image concerning the initial state of the weld.

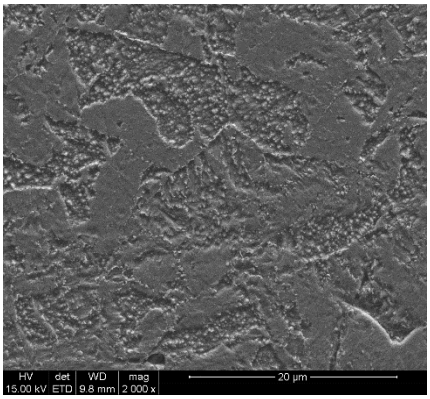

Fig. 4 Parent material – after 5000h of annealing at 600°C

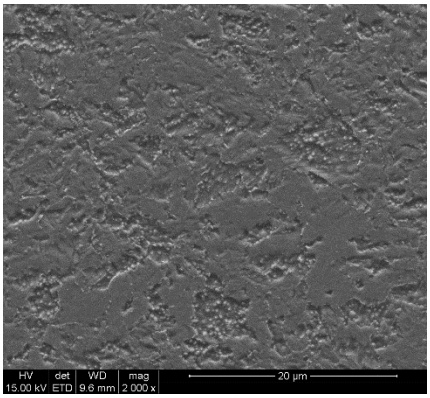

Fig. 5 Heat affected zone – after 5000h of annealing at 600°C

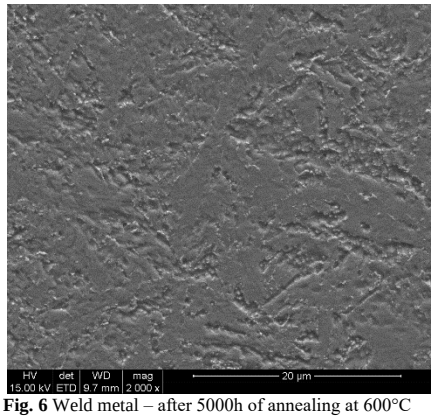

Fig. 6 Weld metal – after 5000h of annealing at 600°C

Welded joint - after annealing for 5000h in 650°C

The microstructure tests of a similar welded joint after annealing at 650ºC were also divided into zones PM/HAZ/WM. Observations of the parent material for both sides of the joint (**Fig. 7**) showed a microstructure similar to the initial state, i.e. the microstructure of tempered strip martensite with a noticeable, slight increase in the size of individual precipitates, mainly along former austenite grain boundaries.

Observations of the microstructure for both sides of the heat-affected zone (**Fig. 8**) showed a fine-grained microstructure of tempered martensite with numerous precipitates on the former austenite grain boundaries and martensite laths. An increase in the size of individual precipitates and their coagulation was observed locally concerning the initial state and annealing at 600ºC.

Microstructure observations for the weld zone (**Fig. 9**) showed that annealing at 650ºC for 5000 hours contributed to a noticeable increase in the precipitates' size and coagulation.

DOI: 10.36547/ams.30.1.1994

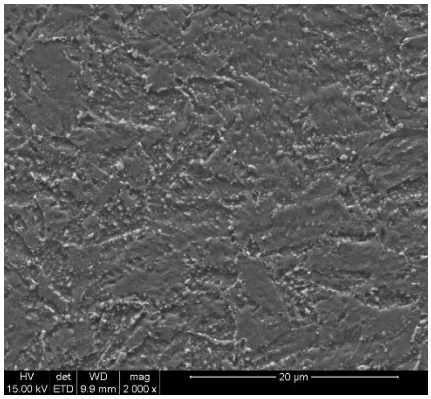

Fig. 7 Parent material – after 5000h of annealing at 650°C

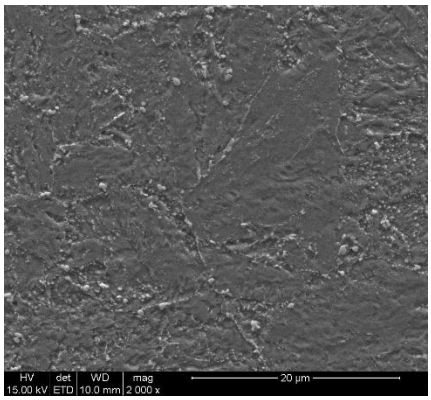

Fig. 8 Heat affected zone – after 5000h of annealing at 650°C

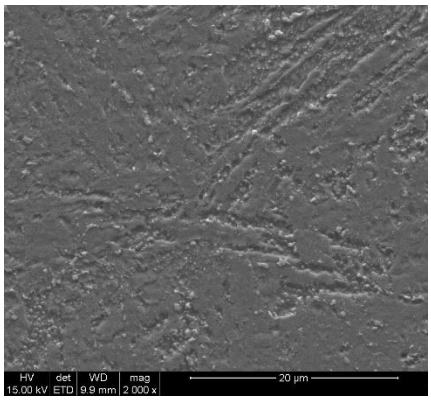

Fig. 9 Weld metal – after 5000h of annealing at 650°C

Welded joint – EDS analysis

The microstructure analysis after annealing, simulating the long-term work of the material, shows us that precipitate changes occur. The changes after annealing concern not only the arrangement but also the size and shape of precipitates. These are shown not only at grain boundaries but also inside them. An example results of one of the performed EDS analyses at a magnification of up to 20,000x indicate that the grain boundary precipitates are rich in chromium, molybdenum, vanadium and tungsten (**Fig. 10**, **Fig. 11**, **Table 2**). The concentrations of individual elements in the material's microstructure indicate the presence of $M_{23}C_6$ and MX precipitates [10]. The result of precipitate analysis is also confirmed by other authors in publications [8,11-13,18-23].

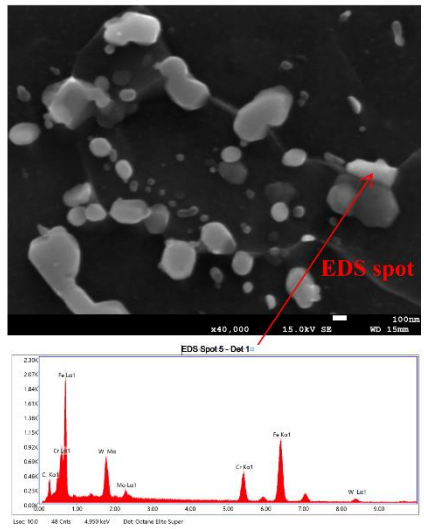

Fig. 10 EDS analysis of specific spot

Table 2 Weight and atomic analysis for described EDS specific spot**.**

Element	Weight %	Atomic %
C	6.54	26.19
W	11.89	3.11
Mo	1.85	0.93
Cr	17.38	16.08
Fe	62.35	53.70

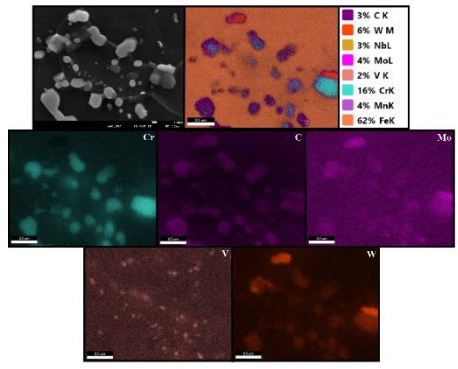

Fig. 11 EDS analysis of tested sample

The average hardness distribution on the cross-sections of the joint for the initial state and after annealing for 5000 h at 600°C and the joint after annealing for 5000 h at 650°C was tested, and it is shown in **Fig. 12**. HV10 values in all zones decreases adequately to the applied annealing conditions in the furnace. The higher the annealing temperature, the more the HV10 hardness values of the tested P92 weldment samples decrease. The result of hardness testing is also confirmed by other authors in publications [14-17].

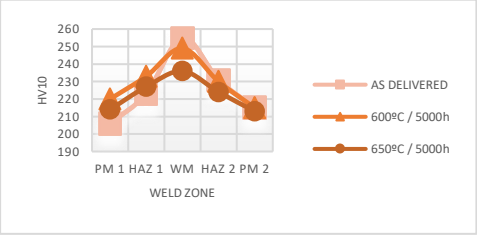

Fig. 12 Hardness HV10 by weld zones and states

CONCLUSIONS

- Microstructure analysis for the parent material zone in the initial and post-annealed state did not show defects (such as microcracks), confirming that the sample welding was done correctly.
- P92 pipe welded joint annealed for 5000h at 600°C and 650°C does not have significant influence for material state. Only small changes in the form of precipitates are observed in the microstructure.
- Annealing for 5000h at 650°C shows a more dynamic increase in the size of the precipitates and their coagulation along grain boundaries of former austenite and martensite laths than annealing for 5000h at 600°C.
- The simulation of the work of the samples in creep conditions reduces the hardness in individual zones of the welded joint adequately to the conditions applied in the furnace.
- The analysis of the image of the concentration of alloying elements indicated that in the microstructure of the tested steel, there are $M_{23}C_6$ type precipitates ($Cr_{23}C_6$, $(Cr,Mo,W)_{23}C_6$), Lavesa phase (Fe_2Mo, Fe_2W) and MX (V(C,N)).

Acknowledgments: Authors are grateful for the support and financing of experimental works by Ministry of Education and Science - Polish Government project: "Doktorat Wdrożeniowy IVth edition".

REFERENCES

1. L. Xinmei, Z. Zhang, Y. Zou, D. Baoshuai, Y. Wei, Z. Yin: IOP Conference Series: Earth and Environmental Science, 358, 2019, 042021. http://dx.doi.org/10.1088/1755-1315/358/4/042021.
2. Y. Hasegawa: Grade 92 creep-strength-enhanced ferritic steel, In: *Coal Power Plant Materials and Life Assessment*, A. Shibli (Ed.), Woodhead Publishing: Cambridge, England 2014, pp. 52–86. http://dx.doi.org/10.1533/9780857097323.1.52.
3. N. Saini, C. Pandey, M.M. Mahapatra, R.S. Mulik: Welding Journal, 2018, 207-213. https://doi.org/10.29391/2018.97.018.
4. J. Parker, J. Siefert: Materials 12(14), 2019, 2257. https://doi.org/10.3390/ma12142257.
5. Y. Wang, R. Kannan, L. Li: Metallurgical and Materials Transactions A, 49(4), 2018, 1264–1275. http://dx.doi.org/10.1007/s11661-018-4490-x.
6. P. Snopinski, M. Król: Metals, 8(11), 2018, 969. https://doi.org/10.3390/met8110969.
7. X. Guo, J. Gong, Y. Jiang, X. Wang, Y. Zhao: Materials at High Temperatures, 32(6), 2015, 566-574. http://dx.doi.org/10.1179/1878641315Y.0000000003.
8. A. Zieliński, R. Wersta, M. Sroka: Archives of Civil and Mechanical Engineering, 22, 2022, 89, http://dx.doi.org/10.1007/s43452-022-00408-6.
9. Ľ. Kaščák, J. Slota, J. Bidulská, R. Bidulský, A. Kubit: Acta Metallurgica Slovaca, 29(4), 2023, 214–218. https://doi.org/10.36547/ams.29.4.1979.
10. G. Golański, A. Zieliński, M. Sroka, J. Słania: Materials, 13, 2020, 1297. https://doi.org/10.3390/ma13061297.
11. N. Saini, R.S. Mulik, M.M. Mahapatra: Materials Science and Engineering A, 716, 2018, 179-188. https://doi.org/10.1016/j.msea.2018.01.035.
12. Y. Shen, H. Liu, Z. Shang, Z. Xu: Journal of Nuclear Materials, 465, 2015, 373-382. https://doi.org/10.1016/j.jnucmat.2015.05.043.
13. F Abe, T Horiuchi, M Taneike, K Sawada: Materials Science and Engineering A, 378, 2004, 299-303. https://doi.org/10.1016/j.msea.2003.11.073.
14. L. Falat, A. Výrostková, V. Homolová, M. Svoboda: Engineering Failure Analysis, 16, 2009, 2114-2120. https://doi.org/10.1016/j.engfailanal.2009.02.004.
15. B. Adhithan, C. Pandey: International Journal of Pressure Vessels and Piping, 192, 2021, 104426. https://doi.org/10.1016/j.ijpvp.2021.104426.
16. LA. Dobrzanski, B. Tomiczek, M. Pawlyta, M. Król: Archives of Metallurgy and Materials, 59(1), 2014, 335-338. https://doi.org/10.2478/amm-2014-0055.
17. J. Obiko, L.H. Chownm, D.J. Whitefield: IOP Conference Series: Materials Science and Engineering, 655, 2019, 01201. http://dx.doi.org/10.1088/1757-899X/655/1/012014.
18. M. Taneike, K. Sawada, F. Abe: Metallurgical and Materials Transactions A, 35, 2004, 1255–1262. https://doi.org/10.1007/s11661-004-0299-x.
19. K. Sawada, K. Sekido, K. Kimura: Materials Characterization, 169, 2020, 110581. https://doi.org/10.1016/j.matchar.2020.110581.
20. F. S. Yin, L.Q. Tian, B. Xue, X. B. Jiang, L. Zhou: Metallurgical and Materials Transactions A, 43, 2012, 2203–2209. https://doi.org/10.1007/s11661-012-1092-x.
21. L. Helis, Y. Toda, T. Hara, H. Miyazaki, F. Abe: Materials Science and Engineering: A, 510–511, 2009, 88-94. https://doi.org/10.1016/j.msea.2008.04.131.
22. A. Kubit, M. Drabczyk, T. Trzepiecinski, W. Bochnowski, Ľ. Kaščák, J. Slota: Metals, 10(5), 2020, 1-18. https://doi.org/10.3390/met10050633.
23. J. Mucha, L. Kascak, E. Spisak: Archives of Civil and Mechanical Engineering, 11(1), 2011, 135-148. https://doi.org/10.1016/S1644-9665(12)60179-4.